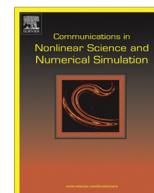




Contents lists available at ScienceDirect

Commun Nonlinear Sci Numer Simulat

journal homepage: [www.elsevier.com/locate/cnsns](http://www.elsevier.com/locate/cnsns)

# A thermodynamically consistent numerical method for a phase field model of solidification

B. Gonzalez-Ferreiro <sup>a,1</sup>, H. Gomez <sup>b</sup>, I. Romero <sup>a,\*</sup>

<sup>a</sup> E.T.S.I. Industriales, Technical University of Madrid, José Gutiérrez Abascal 2, 28006 Madrid, Spain

<sup>b</sup> Department of Mathematical Methods, Universidade da Coruña, Campus de Elviña s/n, 15192 A Coruña, Spain

## ARTICLE INFO

### Article history:

Received 6 November 2012

Received in revised form 21 November 2013

Accepted 21 November 2013

Available online xxxx

### Keywords:

Phase-field

Solidification

Time integration

Nonlinear stability

Structure preservation

## ABSTRACT

A discretization is presented for the initial boundary value problem of solidification as described in the phase-field model developed by Penrose and Fife (1990) [1] and Wang et al. (1993) [2]. These are models that are completely derived from the laws of thermodynamics, and the algorithms that we propose are formulated to strictly preserve them. Hence, the discrete solutions obtained can be understood as discrete dynamical systems satisfying discrete versions of the first and second laws of thermodynamics. The proposed methods are based on a finite element discretization in space and a midpoint-type finite-difference discretization in time. By using so-called discrete gradient operators, the conservation/entropic character of the continuum model is inherited in the numerical solution, as well as its Lyapunov stability in pure solid/liquid equilibria.

© 2013 Elsevier B.V. All rights reserved.

## 1. Introduction

The first widely known mathematical theory of solidification is the so-called Stefan model [3]. This theory is a classical example of free-boundary problem, in which a set of Partial Differential Equations (PDE's) need to be solved on a moving domain. These PDE's are coupled through boundary conditions that hold on an unknown solid–liquid interface. Thus, in the Stefan model the fundamental unknowns are the temperature field and the location of the interface. The attractive feature of this theory is that the temperature defines the phases at each point. Wherever the temperature is lower than the solidification temperature we have the solid phase and vice versa. The interface is defined as the lower-dimension geometrical entity in which the temperature equals the equilibrium temperature.

This paradigm broke down when experimental evidence showed that the temperature on the interface does not equal the solidification temperature. Actually, for static interfaces, the difference between those is proportional to the sum of the principal curvatures of the interface at that point [4]. Several decades later, additional experimental evidence showed that for dynamic interfaces, the difference between the equilibrium temperature and the actual temperature on the interface also depends on the interface velocity (this is normally referred to as kinetic undercooling). These facts clearly showed that temperature was not the right quantity to define the phases, and alternative approaches were sought. This led to the emergence of the phase-field method, in which a new variable called order parameter was introduced to distinguish the phases. The order parameter is defined on the whole domain (both in the liquid and the solid phases) and naturally leads to continuous description of the two-phase system in which diffuse interfaces appear as solutions to the fundamental phase-field

\* Corresponding author. Tel.: +34 91336 3130; fax: +34 91336 3004.

E-mail addresses: [borja.gonzalez@upm.es](mailto:borja.gonzalez@upm.es) (B. Gonzalez-Ferreiro), [hgomez@udc.es](mailto:hgomez@udc.es) (H. Gomez), [ignacio.romero@upm.es](mailto:ignacio.romero@upm.es) (I. Romero).

<sup>1</sup> Tel.: +34 91336 3130; fax: +34 91336 3004.

equations. Therefore, the phase-field method leads not only to a physically sound description of solidification, but also to simpler numerical approximation of the theory, because interface tracking is completely avoided.

There have been several phase-field theories over the years [5–7,2]. We feel that a significant development was the thermodynamic framework for phase-field solidification theories that was developed by Penrose and Fife [1]. In this work, the authors presented a framework to develop phase-field theories that satisfy the fundamental laws of thermodynamics. An example of such a theory was later proposed by Wang et al. [2]. In this paper, we will focus on that theory.

Since modern solidification phase-field theories observe the laws of thermodynamics at the continuous level, it seems desirable to develop numerical algorithms that inherit those properties at the discrete level. This is precisely the objective of this paper. Here we present thermodynamically consistent algorithms that are strictly energy-conserving and entropy-increasing for closed systems. The proposed algorithms are based on our recent work [8–11], which establishes a framework for developing numerical methods that preserve the laws of thermodynamics and symmetries of thermodynamical systems. This idea, which has been previously applied to thermomechanical problems, allows to formulate discrete dynamical systems whose behavior closely resembles that of the corresponding continuum model. Moreover, numerical results indicate that the strict satisfaction of the discrete conservation laws avoids excessive dissipation in the numerical integration which is responsible for the smearing of phase interfaces.

The design of thermodynamically consistent methods ultimately depends on a consistent redefinition of the thermodynamic affinities, in such a way that the correct energy and entropy balance is built, exactly, into the discrete evolution equations. The formulation of such modified derivatives builds upon the so-called discrete gradient operator [12–17], an idea often employed for the design of conserving methods in Hamiltonian mechanics, we, among many others, [18–23]. In the present work, we start from the thermodynamically based phase field model proposed by Wang et al. [2], and further exploit this idea to construct a discretization which inherits the two laws of thermodynamics.

We note that similar ideas have been previously used to derive unconditionally gradient-stable schemes for isothermal phase-field theories, such as, for example, the Cahn–Hilliard equation which governs the phase separation of immiscible fluids [24–26]. In particular, our algorithms have similarities with those proposed by Du and Nicolaides [27]. Some other recent works in this field include [28–32]. However, the aforementioned works focus on algorithms which inherit the dissipation inequality of an isothermal theory, while this paper proposes algorithms which comply with the two laws of thermodynamics in a non-isothermal fully-coupled thermodynamical system.

We are able to prove that the dynamical system defined by Wang's model is Lyapunov stable close to pure phases. This result further indicates that indeed this theory is sound and suitable for the simulation of solidification problems. Moreover, it will be proved that the newly proposed method inherits this nonlinear stability from the continuum problem. Such feature stems from the thermodynamical consistency of the numerical method, and it is not shared by other discretizations.

An outline of the article is the following. In Section 2 the phase field model for solidification due to Penrose and Fife [1] and Wang et al. [2] is summarized. Its numerical approximation is described in Section 3, where standard methods as well as a new discretization are presented. The strict satisfaction of the laws of thermodynamics by the new method is proved. Section 4 analyzes the Lyapunov stability of the continuum model as well as the discrete model, showing again that the numerical solution inherits this desirable feature. Numerical examples of the performance of the new method are addressed in Section 5. Finally, the article concludes with a summary of results in Section 6.

## 2. A phase field model for solidification

Phase field models have proven to be a valid approach for the analytical formulation and numerical solution of solidification problems. In this work we propose a discretization of the model described in [2] in which the phase field equations for a solidification model are derived ensuring that all modeling complies with the two laws of thermodynamics. We summarize in this Section Wang's model, and then in Section 3 we will discretize its equations while preserving the conservation laws.

### 2.1. Balance equations

Consider a solid occupying a volume described by an open set  $V \subset \mathbb{R}^d$ , with  $d = 2$  or  $3$ , and closure  $\bar{V}$ , which includes a solid and a liquid phase. To describe which parts of the body belong to each of the phases, we introduce an order parameter  $\phi : V \rightarrow [0, 1]$  with value  $\phi = 0$  on solid points,  $\phi = 1$  on liquid points, and  $\phi \in (0, 1)$  at the interfaces. In this description, the phase field variable becomes one of the state variables that fully determine the thermodynamic state of every particle of the body.

For every region  $\Omega \subseteq V$ , let  $E(\Omega)$  denote its total energy. Since the energy is an extensive property, it can be expressed as

$$E(\Omega) = \int_{\Omega} e \, d\nu, \quad (1)$$

where  $e$  is the energy density.

If no external power is applied on the body, the first law of thermodynamics states that the total change of energy of any subset  $\Omega$  is due to the thermal power entering through its boundary  $\partial\Omega$ . If  $\mathbf{q} : \bar{V} \rightarrow \mathbb{R}^d$  is the heat flux and  $\mathbf{n}$  is the unit outward normal to the boundary  $\partial\Omega$ , then the first law of thermodynamics reads:

$$\dot{E}(\Omega) = - \int_{\partial\Omega} \mathbf{q} \cdot \mathbf{n} da, \quad (2)$$

where the overdot indicates the time derivative. Applying a standard localization argument, the differential expression of the first law is recovered:

$$\dot{e} = -\nabla \cdot \mathbf{q}. \quad (3)$$

Let  $s : \bar{V} \rightarrow \mathbb{R}^+$  be the bulk entropy density in the body. The total entropy in the two-field body depends on this quantity plus an additional term to account for the interfacial entropy. More precisely, the total entropy of a region  $\Omega \subseteq V$  is denoted as  $S(\Omega)$  and postulated to be of the form:

$$S(\Omega) = \int_{\Omega} \left( s - \frac{\epsilon^2}{2} |\nabla \phi|^2 \right) dv, \quad (4)$$

where  $\epsilon > 0$  is a constant introduced by Wang et al. [2] to modulate the bulk and interface contributions to the entropy.

To study the entropy change during an arbitrary process, let us assume that the entropy density depends on the state variables  $e$  and  $\phi$  and thus  $s = \tilde{s}(e, \phi)$ . Hence

$$\dot{S}(\Omega) = \int_{\Omega} \left( \dot{\tilde{s}} - \epsilon^2 \nabla \dot{\phi} \cdot \nabla \phi \right) dv = \int_{\Omega} \left( \frac{\partial \tilde{s}}{\partial e} \dot{e} + \left( \frac{\partial \tilde{s}}{\partial \phi} + \epsilon^2 \Delta \phi \right) \dot{\phi} - \epsilon^2 \nabla \cdot (\dot{\phi} \nabla \phi) \right) dv. \quad (5)$$

The thermodynamic definition of the temperature field  $T : \bar{V} \rightarrow \mathbb{R}^+$  is

$$T = \left( \frac{\partial \tilde{s}}{\partial e} \right)^{-1}. \quad (6)$$

Using this definition and substituting expression (3) in (5), the entropy rate reads, after integrating by parts, as follows

$$\begin{aligned} \dot{S}(\Omega) &= \int_{\Omega} \left( \frac{-1}{T} \nabla \cdot \mathbf{q} + \left( \frac{\partial \tilde{s}}{\partial \phi} + \epsilon^2 \Delta \phi \right) \dot{\phi} - \epsilon^2 \nabla \cdot (\dot{\phi} \nabla \phi) \right) dv \\ &= \int_{\Omega} \left( \mathbf{q} \cdot \nabla \left( \frac{1}{T} \right) + \left( \frac{\partial \tilde{s}}{\partial \phi} + \epsilon^2 \Delta \phi \right) \dot{\phi} \right) dv - \int_{\partial\Omega} \left( \frac{\mathbf{q}}{T} + \epsilon^2 \dot{\phi} \nabla \phi \right) \cdot \mathbf{n} da. \end{aligned} \quad (7)$$

This equation shows that the total entropy rate is the sum of two contributions. The first contribution collects the entropy production in  $\Omega$  due to heat conduction and internal entropy generation. The second integral in (7) represents the entropy flux entering the region through its boundary.

The Clausius–Planck form of the second principle of thermodynamics states that each of the two terms defining the entropy production of the body must be non-negative. For this to be true, first, a constitutive relation between the heat flux and the temperature must be proposed that guarantees non-negative entropy production from heat conduction. The simplest of such relations is afforded by Fourier's law:

$$\mathbf{q} = M_T \nabla T^{-1}, \quad (8)$$

where  $M_T > 0$  is a function of  $T$ . Under this assumption, the entropy production in  $\Omega$  due to heat conduction can be evaluated to be

$$\int_{\Omega} \mathbf{q} \cdot \nabla T^{-1} dv = \int_{\Omega} M_T |\nabla T^{-1}|^2 dv, \quad (9)$$

which is non-negative. Also, an evolution equation for the phase field parameter is proposed to be

$$\tau \dot{\phi} = \frac{\partial \tilde{s}}{\partial \phi} + \epsilon^2 \Delta \phi, \quad (10)$$

with  $\tau > 0$  controlling the kinetics of  $\phi$ . The internal entropy production then amounts to

$$\int_{\Omega} \left( \frac{\partial \tilde{s}}{\partial \phi} + \epsilon^2 \Delta \phi \right) \dot{\phi} dv = \int_{\Omega} \tau |\dot{\phi}|^2 dv, \quad (11)$$

which again is non-negative. We conclude that a solidification model that employs (8) and (10) satisfies the second law of thermodynamics.

## 2.2. Wang's model for phase field solidification

The evolution equations (3) and (10), together with the constitutive relation (8), define a general model for continua with a phase field state variable. To precisely characterize a solidification model we follow [2], which provides a complete definition of the thermodynamic potentials.

First, let us assume that the internal energy density  $e$  can be expressed as a function of the order parameter and the temperature in the form:

$$e = \hat{e}(\phi, T) = e_L(T) + [p(\phi) - 1]L(T), \quad (12)$$

where  $e_L$  is the internal energy density of the liquid,  $p : [0, 1] \rightarrow \mathbb{R}$  is a polynomial satisfying  $p(0) = 0, p(1) = 1$ . The function  $L(T) = e_L(T) - e_s(T)$  represents the difference between the internal energy densities of the liquid and solid phases at temperature  $T$ . Moreover, let us assume that the temperature dependence of the liquid internal energy density can be written in the simple form

$$e_L(T) = e_L(T_M) + c(T - T_M), \quad (13)$$

where  $c$  is the heat capacity, per unit volume, of the liquid phase, and  $T_M$  is the melting temperature.

To close the model, an expression for the entropy potential needs to be found. For that, let us first obtain the Helmholtz free energy through a Legendre transform of the free energy:

$$f = \hat{f}(\phi, T) = \sup_s (\tilde{e}(\phi, s) - Ts) = \hat{e}(\phi, T) - T\hat{s}(\phi, T), \quad (14)$$

where  $\hat{e}(\phi, T) = \tilde{e}(\phi, \hat{s}(\phi, T))$ . It follows then that

$$\frac{\partial}{\partial T} \left( \frac{\hat{f}(\phi, T)}{T} \right) = \frac{\partial}{\partial T} \left( \frac{\tilde{e}(\phi, \hat{s}(\phi, T))}{T} - \hat{s}(\phi, T) \right) = \frac{-1}{T^2} \hat{e}(\phi, T) + \frac{1}{T} \frac{\partial \tilde{e}}{\partial s} \frac{\partial \hat{s}}{\partial T} - \frac{\partial \hat{s}}{\partial T} = \frac{-1}{T^2} \hat{e}(\phi, T), \quad (15)$$

where we have employed the thermodynamic relation  $T = \frac{\partial \tilde{e}}{\partial s}$ .

The previous expression can be integrated at constant  $\phi$  to yield:

$$\hat{f}(\phi, T) = T \left( \int_{T_M}^T \frac{\hat{e}(\phi, \psi)}{\psi^2} d\psi + \frac{1}{4a} g(\phi) \right), \quad (16)$$

where  $a \in \mathbb{R}^+$  is a constant and  $g : \mathbb{R} \rightarrow \mathbb{R}$  is a function which is chosen to be a double well potential with minima in 0 and 1 to favor pure phases. The constant  $a$  serves to balance the bi-stable contribution  $g$  against the rest of the terms in  $f$ . For simplicity, and without loss of generality, the following potential is proposed:

$$g(\phi) = \phi^2(1 - \phi)^2. \quad (17)$$

Using Eq. (12), the free energy can be re-written as:

$$\hat{f}(\phi, T) = T \left( - \int_{T_M}^T \frac{e_L(\psi)}{\psi^2} d\psi - [p(\phi) - 1]Q(T) + \frac{1}{4a} g(\phi) \right), \quad (18)$$

with the function  $Q$  defined as

$$Q(T) = \int_{T_M}^T \frac{L(\psi)}{\psi^2} d\psi. \quad (19)$$

The integral in (16) can be evaluated in closed form, resulting in:

$$\int_{T_M}^T \frac{e_L(\psi)}{\psi^2} d\psi = \int_{T_M}^T \frac{e_L(T_M) - cT_M}{\psi^2} d\psi + \int_{T_M}^T \frac{c\psi}{\psi^2} d\psi = -[e_L(T_M) - cT_M] \left( \frac{1}{T} - \frac{1}{T_M} \right) + c \ln \left( \frac{T}{T_M} \right). \quad (20)$$

Eqs. (18)–(20) completely define the free energy of the two-phase body. Finally, the expression of the entropy density can be calculated from the internal energy by solving for  $s$  in the definition (14):

$$s = \hat{s}(\phi, T) = \frac{\hat{e}(\phi, T) - \hat{f}(\phi, T)}{T}. \quad (21)$$

The expressions for the functions  $L$  and  $p$  are still open. In [2], two different models are suggested, and we limit our exposition to the model referred to as *model I*. In it, the latent heat  $L$  is assumed to be constant  $L = L_o > 0$  and the polynomial  $p$  is assumed to be:

$$p(\phi) = \phi^3(10 - 15\phi + 6\phi^2). \quad (22)$$

These two expressions close the continuum model of the two-phase solidification problem which, by construction, satisfies the two laws of thermodynamics.

### 3. Space and time discretization

We propose next a full space–time discretization of the evolution problem described in Section 2. To that end, a finite element projection is employed for the spatial discretization and a second order accurate, midpoint-type method for the

time integration. The most salient feature of the proposed approach is that the obtained solution preserves exactly the two laws of thermodynamics, for any time step size. In the case of an isolated volume, for example, energy in the approximated solution is guaranteed to remain constant and total entropy never decreases. This property is crucial for capturing some of the dynamical properties of the continuum problem, as well as endowing the numerical method with an enhanced robustness, especially for stiff problems.

### 3.1. Weak form of the equations

In preparation for a Galerkin discretization of the problem we recast the evolution problem of Section 2 in weak form. As before,  $\phi : V \times [0, T] \rightarrow [0, 1]$  and  $\beta : V \times [0, T] \rightarrow \mathbb{R}^+$  are the order parameter and inverse temperature, respectively, and we assume that the boundary conditions

$$\phi(x, t) = \bar{\phi}(x, t) \quad \text{on } \partial_\phi V, \quad \beta(x, t) = \bar{\beta}(x, t) \quad \text{on } \partial_\beta V \quad (23)$$

are known, where  $\partial_\phi V$  and  $\partial_\beta V$  are parts of the boundary of  $V$ . Consider the trial functional spaces

$$\begin{aligned} \mathcal{S} &:= \left\{ \phi \in C^1((0, T); H^1(V)), \phi = \bar{\phi} \text{ on } \partial_\phi V \right\}, \\ \mathcal{U} &:= \left\{ \beta \in C^1((0, T); H^1(V)), \beta = \bar{\beta} \text{ on } \partial_\beta V \right\} \end{aligned} \quad (24)$$

and the corresponding spaces of test functions

$$\begin{aligned} \mathcal{T} &:= \left\{ \psi \in C^1((0, T); H^1(V)), \psi = 0 \text{ on } \partial_\phi V \right\} \\ \mathcal{V} &:= \left\{ \mu \in C^1((0, T); H^1(V)), \mu = 0 \text{ on } \partial_\beta V \right\}. \end{aligned} \quad (25)$$

The order parameter  $\phi \in \mathcal{S}$  and (inverse) temperature  $\beta \in \mathcal{U}$  satisfy the weak form of the energy balance equation and the evolution of the order parameter if

$$\begin{aligned} \left\langle \frac{\partial \hat{e}}{\partial \phi} \dot{\phi} + \frac{\partial \hat{e}}{\partial \beta} \dot{\beta}, \psi \right\rangle &= \langle M_T \nabla \beta, \nabla \psi \rangle, \\ \langle \tau \dot{\phi}, \mu \rangle &= \left\langle \frac{\partial \hat{s}}{\partial \phi}, \mu \right\rangle - \langle \epsilon^2 \nabla \phi, \nabla \mu \rangle \end{aligned} \quad (26)$$

for all  $(\psi, \mu) \in \mathcal{T} \times \mathcal{V}$ , at every instant  $t \in (0, T)$ . To complete the formulation of the problem, these variational need to be complemented with the initial conditions:

$$\phi(x, 0) = \phi_0(x), \quad \beta(x, 0) = \beta_0(x) \quad (27)$$

for all  $x \in V$ . We note that, abusing the notation, we have employed the symbols  $\hat{e}$  and  $\hat{s}$  to denote, respectively, the energy and entropy density functions of the order parameter and inverse temperature, where in Section 2 the temperature itself was the argument.

### 3.2. Standard discretization

We proceed to discretize Eq. (26) in space and time. Starting with the spatial discretization, we consider a triangulation of the domain  $V = \cup_{e \in \mathcal{N}} V_e$  into elements  $V_e$ , connecting the set of nodes  $\mathcal{N}$ . Also, the time interval  $[0, T]$  is partitioned into sub-intervals  $[t_n, t_{n+1})$ , with  $0 = t_0 < t_1 < \dots < t_N = T$  and  $\Delta t = t_{n+1} - t_n$ , assumed for simplicity to be constant. Then, the following finite dimensional spaces are defined:

$$\begin{aligned} \mathcal{S}_n^h &= \left\{ \phi_n^h(x) = \sum_{a \in \mathcal{N}} N^a(x) \phi_n^a, \phi_n^h(x) = \bar{\phi}(x, t_n) \text{ on } \partial_\phi V \right\}, \\ \mathcal{U}_n^h &= \left\{ \beta_n^h(x) = \sum_{a \in \mathcal{N}} N^a(x) \beta_n^a, \beta_n^h(x) = \bar{\beta}(x, t_n) \text{ on } \partial_\beta V \right\} \end{aligned} \quad (28)$$

and

$$\begin{aligned} \mathcal{T}^h &= \left\{ \psi_n^h(x) = \sum_{a \in \mathcal{N}} N^a(x) \psi_n^a, \psi_n^h(x) = 0 \text{ on } \partial_\phi V \right\}, \\ \mathcal{V}^h &= \left\{ \mu_n^h(x) = \sum_{a \in \mathcal{N}} N^a(x) \mu_n^a, \mu_n^h(x) = 0 \text{ on } \partial_\beta V \right\}, \end{aligned} \quad (29)$$

to approximate the test and trial spaces, respectively. In all the definitions,  $N^a, a \in \mathcal{N}$  refer to the standard isoparametric interpolation functions. The evolution problem (26) can then be approximated by solving for the discrete state variables  $(\phi_n^h, \beta_n^h) \in \mathcal{S}_n^h \times \mathcal{U}_n^h$  in the system of algebraic equations:

$$\begin{aligned} \left\langle \frac{\partial \hat{e}}{\partial \phi} \frac{\phi_{n+1}^h - \phi_n^h}{\Delta t} + \frac{\partial \hat{e}}{\partial \beta} \frac{\beta_{n+1}^h - \beta_n^h}{\Delta t}, \psi^h \right\rangle &= \left\langle M_T \nabla \beta_{n+\frac{1}{2}}^h, \nabla \psi^h \right\rangle, \\ \left\langle \tau \frac{\phi_{n+1}^h - \phi_n^h}{\Delta t}, \mu^h \right\rangle &= \left\langle \frac{\partial \hat{s}}{\partial \phi}, \mu^h \right\rangle - \left\langle \epsilon^2 \nabla \phi_{n+\frac{1}{2}}^h, \nabla \mu^h \right\rangle \end{aligned} \quad (30)$$

for all  $(\psi^h, \mu^h) \in \mathcal{T}^h \times \mathcal{V}^h$  which satisfy the initial conditions

$$\phi_0^h(x) = \phi_0(x), \quad \beta_0^h(x) = \beta_0(x). \quad (31)$$

In Eq. (26), the partial derivatives  $\frac{\partial \hat{e}}{\partial \phi}$ ,  $\frac{\partial \hat{e}}{\partial \beta}$ ,  $\frac{\partial \hat{s}}{\partial \phi}$ , must be evaluated at the midpoint state defined as

$$(\phi_{n+\frac{1}{2}}^h, \beta_{n+\frac{1}{2}}^h) := \frac{1}{2} [(\phi_n^h, \beta_n^h) + (\phi_{n+1}^h, \beta_{n+1}^h)]. \quad (32)$$

Finally, we note that in the definition of the boundary and initial values of the trial functions, the trial functions are set equal to the projection of the known data onto the finite element space.

### 3.3. A thermodynamically consistent discretization

The discretization (30) is standard, and it is well-known that has second order accuracy in time. Despite its simplicity, the solution obtained with it does not satisfy the laws of thermodynamics in the discrete setting; even for a closed system, the total energy need not remain constant and the total entropy need not increase. In view of the importance of preserving these two principles, we propose next a modification of (30) which will provide approximations that preserve unconditionally the two laws of thermodynamics.

#### 3.3.1. The discrete derivative

The discrete derivative (or discrete gradient) is an expression that approximates the derivative operator and which has been often employed in the formulation of conserving methods. See, among many others, [18–20,33,17,21,22]. The idea, which can be found originally in [12–15], essentially consists in a consistent approximation of the derivative which satisfies a property, commonly referred to as directionality, and described below.

The discrete derivative can be defined on real functions defined on the real line, but also on more general tensor fields. Moreover, there is not a unique definition, but an equivalent class of discrete derivatives [34–36]. We summarize next the simplest definition for real valued functions of two variables, which will be employed in the design of a consistent algorithm next.

Given a differentiable function  $f: \mathbb{R} \rightarrow \mathbb{R}$  and  $a, b \in \mathbb{R}$ , its derivative  $f'$  at  $(a+b)/2$  can be approximated by a “discrete derivative”  $Df: \mathbb{R} \times \mathbb{R} \rightarrow \mathbb{R}$  defined as:

$$Df(a, b) := \frac{f(b) - f(a)}{b - a}. \quad (33)$$

This is a second order approximation to  $f'(\frac{a+b}{2})$  which satisfies the so-called directionality property:

$$Df(a, b) \cdot (b - a) = f(b) - f(a) \quad (34)$$

and has the well-defined limit:

$$\lim_{b \rightarrow a} Df(a, b) = f'(a). \quad (35)$$

Next we extend the discrete derivative operator to differentiable functions on  $\mathbb{R}^2$ , which is the case of interest for the phase field problem, noting that the extension to  $\mathbb{R}^n$  follows the same arguments. Let  $g: \mathbb{R}^2 \rightarrow \mathbb{R}$ ; given two points  $(x_1, y_1), (x_2, y_2) \in \mathbb{R}^2$ , the partial discrete derivatives of  $g$  with respect to its two arguments are denoted

$$D_1 g: \mathbb{R}^2 \times \mathbb{R}^2 \rightarrow \mathbb{R}, \quad D_2 g: \mathbb{R}^2 \times \mathbb{R}^2 \rightarrow \mathbb{R} \quad (36)$$

and defined as:

$$\begin{aligned} D_1 g(x_1, y_1, x_2, y_2) &= \frac{g(x_2, y_1) - g(x_1, y_1) + g(x_2, y_2) - g(x_1, y_2)}{2(x_2 - x_1)}, \\ D_2 g(x_1, y_1, x_2, y_2) &= \frac{g(x_1, y_2) - g(x_1, y_1) + g(x_2, y_2) - g(x_2, y_1)}{2(y_2 - y_1)}. \end{aligned} \quad (37)$$

These two functions are second order approximations to the corresponding partial derivatives of  $g$  at the midpoint  $(\frac{x_1+x_2}{2}, \frac{y_1+y_2}{2})$  and satisfy the directionality property:

$$D_1 g(x_1, y_1, x_2, y_2)(x_2 - x_1) + D_2 g(x_1, y_1, x_2, y_2)(y_2 - y_1) = g(x_2, y_2) - g(x_1, y_1). \quad (38)$$

Furthermore, they are well-defined in the limits:

$$\begin{aligned}\lim_{x_2 \rightarrow x_1} D_1 g(x_1, y_1, x_2, y_2) &= \frac{1}{2} \left( \frac{\partial g}{\partial x}(x_1, y_1) + \frac{\partial g}{\partial x}(x_1, y_2) \right), \\ \lim_{y_2 \rightarrow y_1} D_2 g(x_1, y_1, x_2, y_2) &= \frac{1}{2} \left( \frac{\partial g}{\partial y}(x_1, y_1) + \frac{\partial g}{\partial y}(x_2, y_1) \right).\end{aligned}\quad (39)$$

### 3.3.2. Structure preserving discretization

We propose next a modification of the midpoint rule (30) which will strictly preserve the laws of thermodynamics. For that, let

$$\mathcal{W}^h = \left\{ w^h(x) = \sum_{a \in \mathcal{N}} N^a(x) w^a \right\} \quad (40)$$

and define two new finite element functions  $e_n^h \in \mathcal{W}^h$  and  $\omega_n^h \in \mathcal{W}^h$  obtained by the  $L_2$  projections:

$$\begin{aligned}\langle e_n^h, v^h \rangle &= \langle \hat{e}(\phi_n^h, \beta_n^h), v^h \rangle, \\ \langle \beta_n^h, \eta^h \rangle &= \langle D_e \tilde{S}(\phi_n^h, e_n^h, \phi_{n+1}^h, e_{n+1}^h), \eta^h \rangle\end{aligned}\quad (41)$$

for all  $v^h$  and  $\eta^h$  in  $\mathcal{W}^h$ . The partial derivative  $\frac{\partial \tilde{S}}{\partial e}$  corresponds physically to the inverse temperature  $\omega$ , so the second projection in (41) defines an algorithmic approximation to this field. By employing these two new functions, we propose to replace (30) by the numerical scheme:

$$\begin{aligned}\left\langle \frac{e_{n+1}^h - e_n^h}{\Delta t}, \psi^h \right\rangle &= \langle M_T \nabla \beta_n^h, \nabla \psi^h \rangle, \\ \left\langle \tau \frac{\phi_{n+1}^h - \phi_n^h}{\Delta t}, \mu^h \right\rangle &= \langle D_\phi \tilde{S}(\phi_n^h, e_n^h, \phi_{n+1}^h, e_{n+1}^h), \mu^h \rangle - \langle \epsilon^2 \nabla \phi_{n+\frac{1}{2}}^h, \nabla \mu^h \rangle\end{aligned}\quad (42)$$

for all  $(\psi^h, \mu^h) \in \mathcal{T}^h \times \mathcal{V}^h$ . The complete solution of the problem requires, at every time step, solving (41) and (42) for  $(\phi_{n+1}^h, \beta_{n+1}^h, e_{n+1}^h, \omega_{n+1}^h)$ , with the initial conditions

$$\phi_0^h(x) = \phi_0(x), \quad \beta_0^h(x) = \beta_0(x), \quad e_0^h = \hat{e}(\phi_0^h, \beta_0^h). \quad (43)$$

As explained below, the computational effort of such a solution is almost identical to that of the standard (midpoint) method.

Let the total energy and entropy of the discrete solution and the time instant  $t_n$  be defined, respectively, as:

$$E_n = \int_V \hat{e}(\phi_n^h, \beta_n^h) dv, \quad S_n = \int_V \left( \hat{s}(\phi_n^h, \beta_n^h) - \frac{\epsilon^2}{2} |\nabla \phi_n^h|^2 \right) dv. \quad (44)$$

Then, the next result follows:

**Theorem 3.1.** *The space–time discretization given by (41) and (42) is a second order accurate method in time which exactly preserves the laws of thermodynamics. That is, for a closed volume  $V$  the following holds:*

$$E_{n+1} = E_n, \quad S_{n+1} \geq S_n. \quad (45)$$

**Proof.** The accuracy of the discretization is a direct consequence of the accuracy of the forward difference quotients and the accuracy of the discrete differential operator.

To prove the conservation of energy, let select the test function  $\psi^h$  to be identically 1. Then, the right hand side of Eq. (42)<sub>1</sub> vanishes. This, in turn, implies

$$0 = \left\langle \frac{e_{n+1}^h - e_n^h}{\Delta t}, 1 \right\rangle = \left\langle \frac{e(\phi_{n+1}^h, \beta_{n+1}^h) - e(\phi_n^h, \beta_n^h)}{\Delta t}, 1 \right\rangle = \frac{E_{n+1} - E_n}{\Delta t}, \quad (46)$$

which is the discrete statement of the first law of thermodynamics.

To show the validity of the second law, we select  $\mu^h = \phi_{n+1}^h - \phi_n^h$  in (42)<sub>2</sub> to obtain:

$$\begin{aligned}\tau \frac{\|\phi_{n+1}^h - \phi_n^h\|^2}{\Delta t} &= \langle D_\phi \tilde{S}, \phi_{n+1}^h - \phi_n^h \rangle - \left\langle \frac{\epsilon^2}{2} (\nabla \phi_{n+1}^h + \nabla \phi_n^h), \nabla \phi_{n+1}^h - \nabla \phi_n^h \right\rangle \\ &= \langle D_\phi \tilde{S}, \phi_{n+1}^h - \phi_n^h \rangle - \frac{\epsilon^2}{2} (\|\nabla \phi_{n+1}^h\|^2 - \|\nabla \phi_n^h\|^2) + \langle D_e \tilde{S}, e_{n+1}^h - e_n^h \rangle - \langle D_e \tilde{S}, e_{n+1}^h - e_n^h \rangle \\ &= S_{n+1} - S_n - \langle D_e \tilde{S}, e_{n+1}^h - e_n^h \rangle.\end{aligned}\quad (47)$$

The last term of the right hand side can be evaluated using the projection (41)<sub>2</sub> and the evolution equation (42)<sub>1</sub> to yield:



$$\langle D_e \tilde{s}, e_{n+1}^h - e_n^h \rangle = \langle \beta_*^h, e_{n+1}^h - e_n^h \rangle = \Delta t \langle \nabla \beta_*^h, M_T \nabla \beta_*^h \rangle. \quad (48)$$

This quantity is non-negative always, and we can conclude that

$$S_{n+1} - S_n = \tau \frac{\|\phi_{n+1}^h - \phi_n^h\|^2}{\Delta t} + \Delta t \langle \nabla \beta_*^h, M_T \nabla \beta_*^h \rangle \geq 0, \quad (49)$$

proving the last part of the theorem.  $\square$

The method (42) is second order accurate (in time), rigorously preserves the two laws of thermodynamics but, when compared with the standard midpoint rule, it requires the solution of two additional finite element functions  $e_n^h$  and  $\omega_n^h$ . However, the two new variables are obtained by the simple projection (41), and can be solved by factorizing the Gram matrix with components

$$M_{ab} = \langle N_a, N_b \rangle. \quad (50)$$

This is the projection matrix for both the energy and the inverse temperature, and it is constant, so it can be factorized just once at the beginning of the simulation and re-used at every time step.

In our implementation, the equations of the method (41) and (42) are solved in a staggered fashion. First, the projections (41) are employed to update  $(e_{n+1}^h, \beta_{n+1}^h)$ . Then, the balance equations (42) are solved for  $(\phi_{n+1}^h, \beta_{n+1}^h)$ , repeating this two steps until the convergence of the four fields. In this way, since the cost of the projections is negligible, the final cost of the method is only slightly greater than that of the midpoint rule.

#### 4. Dynamic stability analysis

The numerical method (42) defines a solution sequence  $\{\phi_n^h, \beta_n^h, e_n^h, \beta_*^h\}_{n=0}^N$ . In contrast with discretizations such as the midpoint rule (30), the thermodynamic consistency of the newly proposed method endows it with a notion of nonlinear stability to be described next.

Before discussing the stability of the proposed method we show first that indeed, the initial boundary value problem defined by (26) is stable, in the sense of Lyapunov, at equilibrium points with a purely solid or liquid phase. Later we will prove that the same stability estimate is inherited by the thermodynamically consistent method.

**Theorem 4.1.** *The dynamical system defined by (26) and Wang's thermodynamical potentials is stable, in the sense of Lyapunov, at equilibrium points in which all the body is either completely solid or liquid.*

**Proof.** Let  $(\bar{\phi}, \bar{\beta}) \in [H_0^1(V)]^2$  be an equilibrium point of the dynamical system defined by (26) and let  $\omega_M := T_M^{-1}$ . The function  $\bar{\phi}$  is constant with value 0 or 1, and the function  $\bar{\omega}$  is a constant inverse temperature field such that, when  $\bar{\phi} \equiv 0$  then  $\bar{\beta} > \beta_M$ . Likewise, when the volume contains only liquid in equilibrium, i.e.  $\bar{\phi} \equiv 1$ , the inverse temperature must satisfy  $\bar{\beta} < \beta_M$ .

Consider the functionals  $\mathcal{F} : [H_0^1]^2 \rightarrow C^1(0, T)$

$$\mathcal{F}[\phi, \beta] := \int_V \left[ \hat{e}(\phi, \beta) - \bar{\beta}^{-1} \left( \hat{s}(\phi, \beta) - \frac{\epsilon^2}{2} |\nabla \phi|^2 \right) \right] dV \quad (51)$$

and  $\mathcal{L} : [H_0^1]^2 \rightarrow C^1(0, T)$

$$\mathcal{L}[\phi, \omega] := \mathcal{F}[\phi, \beta] - \mathcal{F}[\bar{\phi}, \bar{\beta}]. \quad (52)$$

We claim that  $\mathcal{L}$  is a Lyapunov functional for the dynamics of the solidification problem. The functional  $\mathcal{F}$  can be interpreted as the Helmholtz free energy of the system, obtained by subtracting from the internal energy the entropy multiplied by the temperature. Thus, the stability estimate is equivalent to the statement that, when close to equilibria, the free energy will evolve towards minima.

To show that  $\mathcal{L}$  is indeed a Lyapunov function, we start by noting that  $\mathcal{L}(\bar{\phi}, \bar{\omega}) = 0$ . Moreover, the value of  $\mathcal{L}$  never increases along trajectories starting away from the equilibrium point. To see that, let  $(\phi, \beta) \neq (\bar{\phi}, \bar{\beta})$ . Then

$$\dot{\mathcal{L}}[\phi, \omega] = \dot{\mathcal{F}}[\phi, \omega] = \dot{E} - \bar{\beta}^{-1} \dot{S} \leq 0, \quad (53)$$

where the last inequality follows from the two laws of thermodynamics. Finally, we show that there exists a neighborhood of  $(\bar{\phi}, \bar{\omega})$  in which the functional (52) bounds from above a norm of the solution:

$$\mathcal{L}[\phi, \beta] \geq C \left( \|\phi - \bar{\phi}\|_{H_0^1(V)} + \bar{\beta}^{-1} \|\beta - \bar{\beta}\|_{L_2(V)} \right), \quad (54)$$

where  $C > 0$  is a constant independent of  $(\phi, \beta)$ .

The proof of this last assertion depends on the specific form of the internal energy and entropy in Wang's model and we consider the case  $\bar{\phi} \equiv 0, \bar{\beta} > \beta_M$  corresponding to a fully solid phase. A straightforward manipulation of the expression  $\mathcal{L}[\phi, \beta]$  for Wang's model allows to split the Lyapunov function as



$$\mathcal{L}[\phi, \beta] = \mathcal{L}_\phi[\phi] + \mathcal{L}_\omega[\beta], \quad (55)$$

with

$$\begin{aligned} \mathcal{L}_\phi[\phi] &:= \int_V \left( \frac{1}{4a\beta} g(\phi) + L_o \frac{\bar{\beta} - \beta_M}{\beta} p(\phi) \right) dV + \frac{\epsilon^2}{2\beta} |\phi|_1^2, \\ \mathcal{L}_\beta[\beta] &:= \frac{c}{\beta} \int_V \left( \frac{\bar{\beta}}{\beta} - 1 - \log(\bar{\beta}/\beta) \right) dV. \end{aligned} \quad (56)$$

The functions  $p$  and  $g$  are in  $C^\infty(\mathbb{R})$  and satisfy

$$p(0) = g(0) = p'(0) = g'(0) = 0, \quad p''(0) > 0, \quad g''(0) > 0. \quad (57)$$

Thus there exists a constant  $C$  such that  $g(\phi) \geq C|\phi|^2$ ,  $p(\phi) \geq C|\phi|^2$  in a neighborhood of  $\phi = 0$  and thus

$$\mathcal{L}_\phi[\phi] \geq \int_V C|\phi|^2 dV + \frac{\epsilon^2}{2\beta} |\phi|_1^2 \geq C\|\phi\|_{H_0^1(V)}^2. \quad (58)$$

A similar argument can be followed to bound the term  $\mathcal{L}_\omega$ . In this case, the integrand of (56)<sub>2</sub> can be written as

$$\frac{c}{\beta} \left( \frac{\bar{\beta}}{\beta} - 1 - \log(\bar{\beta}/\beta) \right) = \frac{c}{\beta} h\left(\frac{\beta - \bar{\beta}}{\beta}\right), \quad (59)$$

with  $h: \mathbb{R} \rightarrow \mathbb{R}$  defined as

$$h(x) = \frac{1}{1+x} - 1 + \log(1+x). \quad (60)$$

This function satisfies  $h(0) = h'(0) = 0$  and  $h''(0) > 0$ , thus, as before, there exists a constant  $C$  such that  $h(x) \geq C|x|^2$  and we conclude

$$\mathcal{L}_\beta[\beta] \geq \frac{c}{\beta} \int_V C \left| \frac{\beta - \bar{\beta}}{\beta} \right|^2 dV \geq \frac{C}{\beta} \|\beta - \bar{\beta}\|_{L_2(V)}^2. \quad (61)$$

This bound and (58) show that  $\mathcal{L}$  is indeed a Lyapunov function for the equilibrium at  $\phi \equiv 0$  and thus the solution is nonlinearly stable at this point.

The analysis of the Lyapunov stability close to the purely liquid phase (corresponding to  $\bar{\phi} \equiv 1$  and  $\bar{\beta} < \beta_M$ ) is completely analogous to the one presented and details are omitted.  $\square$

The thermodynamic consistent method presented in this work inherits the stability of Wang's model:

**Theorem 4.2.** *The discrete dynamical system (42) applied to Wang's model is dynamically stable in the sense of Lyapunov, i.e. the value of the functional (52) evolves as in*

$$\mathcal{L}(\phi_{n+1}^h, \beta_{n+1}^h) \leq \mathcal{L}(\phi_n^h, \beta_n^h). \quad (62)$$

Moreover, the norms of the auxiliary fields  $e_n^h$  and  $\beta_n^h$  remain bounded at all times close to equilibrium points.

**Proof.** The increase in the value of the Lyapunov functional follows directly from the discrete conservation/dissipation properties of the method. Furthermore, close to an equilibrium point, the Lyapunov functional bounds the norm of the solution  $(\phi_n^h, \beta_n^h)$  at all times. Finally, since the auxiliary fields  $e_n^h$  and  $\beta_n^h$  are obtained from  $L_2$  projections it follows that

$$\|e_n^h\|_{L_2(V)} \leq \|\hat{e}(\phi_n^h, \beta_n^h)\|_{L_2(V)}, \quad \|\beta_n^h\|_{L_2(V)} \leq \|D_e \tilde{S}(\phi_n^h, e_n^h, \phi_{n+1}^h, e_{n+1}^h)\|_{L_2(V)} \quad (63)$$

and thus both must remain bounded since the energy and discrete entropy are continuous functions of their (bounded) arguments.  $\square$

The nonlinear dynamical stability of the proposed discretization is not shared by the midpoint rule, since it crucially depends on the discrete conservation/dissipation properties of the method.

## 5. Simulations

We illustrate next, by means of numerical simulations, the behavior of the proposed numerical discretization and we compare it with a standard formulation based on finite elements in space and the midpoint rule in time. To showcase the features of the proposed method, first a simulation will be presented to show the differences in the evolution of the energy and entropy in the compared methods. A second example will show that even small deviations from thermodynamical consistency can lead to quite different dendritic patterns. All the simulations have been run in a finite element code developed by the authors.

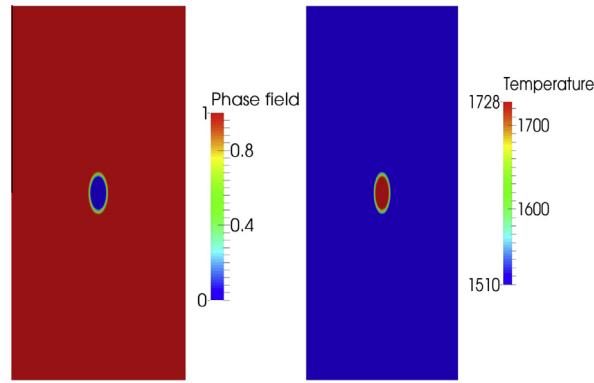


**Fig. 1.** Initial conditions on the phase field (left) and temperature (right). The whole region is initially in the liquid phase at a temperature  $T_o = T_m - 217$  K, except for an ellipsoidal region in the center which is in the solid phase at the melting temperature.

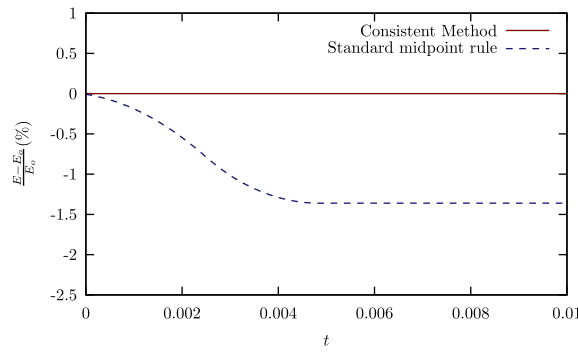


**Fig. 2.** Relative energy evolution in Example 5.1.

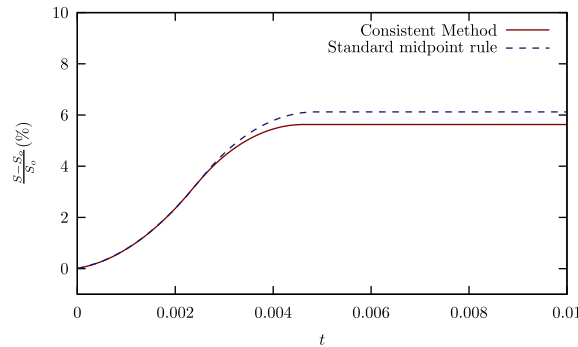


**Fig. 3.** Relative entropy evolution in Example 5.1.

In both simulations we consider the solidification of pure nickel in a completely isolated region. The thermodynamic properties of this material have been obtained from [37]: the interfacial energy is  $\sigma = 3.7 \times 10^{-5}$  J/cm<sup>2</sup>, the melting temperature is  $T_m = 1728$  K, the latent heat per unit volume is  $L_o = 2350$  J/cm<sup>3</sup>, the heat capacity per unit volume is  $c = 5.42$  J/K cm<sup>3</sup>, the thermal diffusivity is  $\kappa = 0.155$  cm<sup>2</sup>/s, and the interfacial mobility is  $\mu = 285$  cm/K s.

All these physical quantities do not suffice to model the behavior of dendrites. It is expected that the tip radius of the dendrites to be significantly smaller than the characteristic length scale of the domain, while still remaining considerably larger than the interface thickness.

We relate the length scale of the domain  $\lambda$  to the parameters governing the interface dynamics and characterizing the size of dendrites, through a non-dimensional parameter  $\alpha$  defined as:

$$\alpha = \frac{\sqrt{2} L_o^2}{12 c \sigma T_m} \lambda. \quad (64)$$

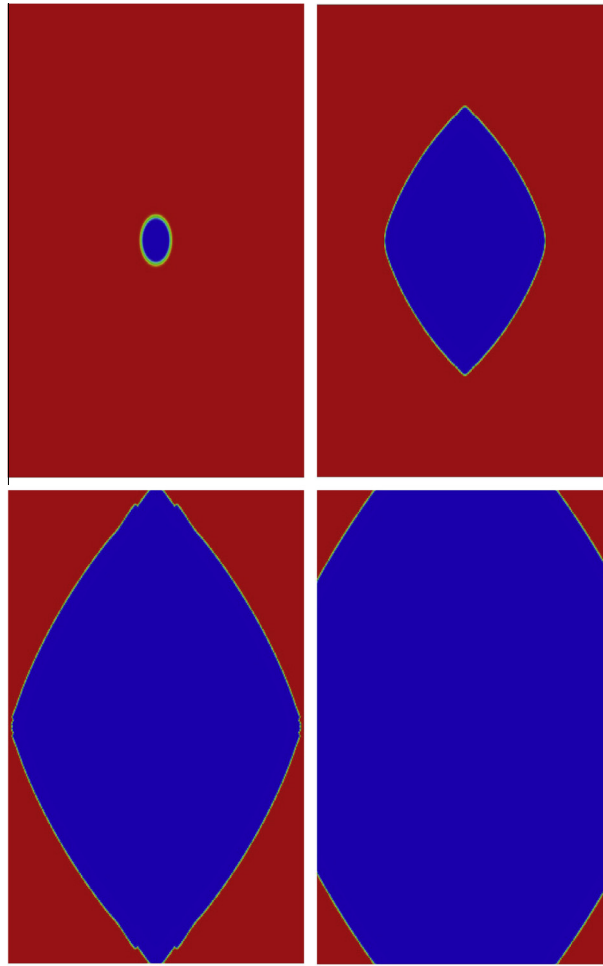


**Fig. 4.** Phase field plots in the solution obtained with the thermodynamically consistent method (red = liquid, blue = solid). From top to bottom, left to right, snapshots correspond to time instants  $t = 0.0, 1.25, 2.5, 3.75$  ms. Approximately at time  $t = 4.5$  ms the whole domain solidifies. (For interpretation of the references to colour in this figure caption, the reader is referred to the web version of this article.)

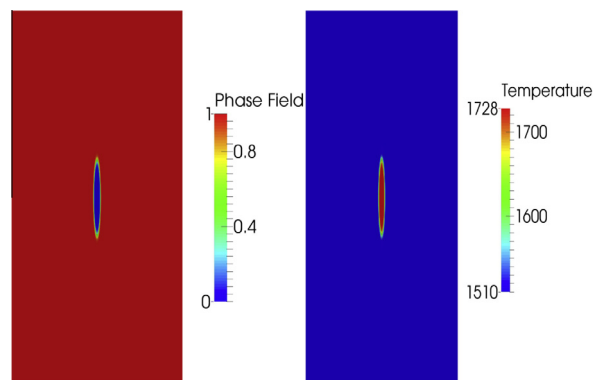


**Fig. 5.** Initial conditions on the phase field (left) and temperature (right). The whole region is initially in the liquid phase at a temperature  $T_o = T_m - 217$  K, except for an ellipsoidal region in the center which is in the solid phase at the melting temperature.

Similarly, we introduce another non-dimensional parameter  $\tilde{\epsilon}$ , defined as the ratio between the length scale and the thickness of the interface:

$$\tilde{\epsilon} = \frac{\delta}{\lambda}. \quad (65)$$

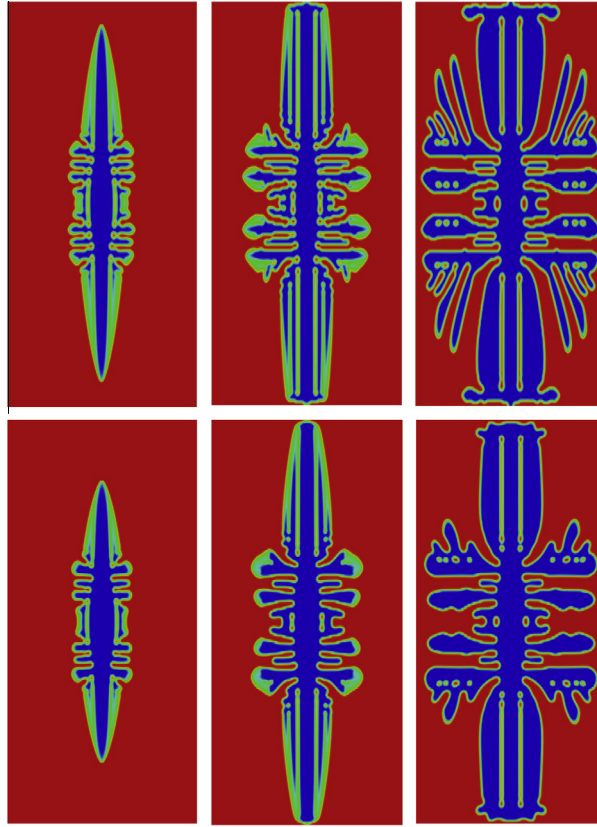


**Fig. 6.** Phase field plots obtained with the thermodynamically consistent method (top) and midpoint rule (bottom) at instants (from left to right)  $t = 0.05$  s,  $t = 0.10$  s, and  $t = 0.20$  s.

In our simulations, we want to model interfaces whose thickness are smaller than the dendritic structures while, at the same time, this thickness need to be large enough that the finite element mesh can resolve it accurately. Hence, we have fixed  $\alpha = 400$  and  $\tilde{\epsilon} = 0.005$ , as suggested by Wheeler et al. [37]. From the given physical constants and the non-dimensional parameters, all the remaining constants of the model can be calculated. In particular, the constants  $\tau$  and  $\epsilon$  appearing in Eq. (42) and  $a$ , in Eq. (18), have expressions:

$$\tau = \frac{72 \alpha c \sigma \tilde{\epsilon}}{\mu T_m L_o}, \quad \epsilon^2 = \frac{72 \tilde{\epsilon} c \alpha \sigma^2}{L_o^2}, \quad a = \frac{\tilde{\epsilon} c \alpha T_m^2}{L_o^2}. \quad (66)$$

### 5.1. Complete solidification of a liquid body

In this example we study the evolution of an undercooled nickel body with a small elliptic region already in solid phase at the melting temperature. While the body is  $0.43 \times 0.21$  mm<sup>2</sup>, the major and minor radii of the ellipse measure respectively 43  $\mu$ m and 21  $\mu$ m. The solid is discretized uniformly resulting in a mesh of  $200 \times 200$  elements. The initial temperature and phase fields are displayed in Fig. 1.

A reduced latent heat  $L_o = 1450$  J/cm<sup>3</sup> is employed in this simulation to accentuate the differences in the solutions obtained by the compared discretizations. In this example, the complete domain solidifies and dendrites do not appear.

As shown in Figs. 2 and 3, when the thermodynamically consistent method is employed the energy is exactly preserved and the entropy increases. In contrast, when the standard midpoint rule is used, a non-physical energy growth appears. This growth stops when the full region solidifies and a steady state is attained. See Fig. 4 for an illustration of the solidification process.

### 5.2. Dendritic growth during nickel solidification

In this second simulation we study the dendritic growth during the solidification of an undercooled nickel region. The initial temperature of the liquid phase is 217 K below the melting temperature. The initial phase and temperature fields

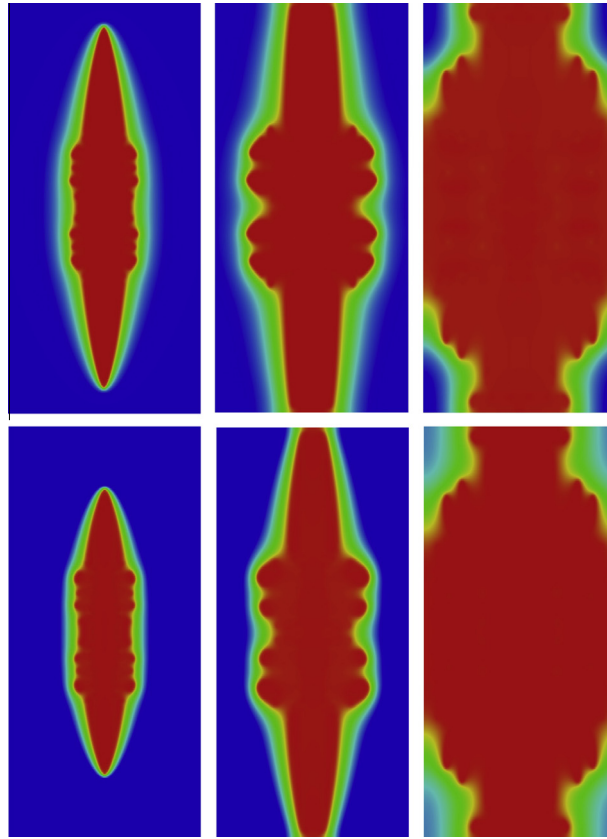


**Fig. 7.** Temperature plots obtained with the thermodynamically consistent method (top) and midpoint rule (bottom) at instants (from left to right)  $t = 0.05$  s,  $t = 0.10$  s, and  $t = 0.20$  s.

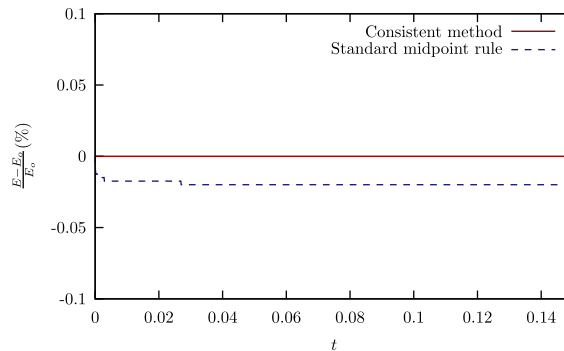


**Fig. 8.** Relative energy evolution in Example 5.2.

are depicted in Fig. 5. The spatial discretization is the same as in the example of Section 5.1 although the dimensions of the body and the initial elliptic region are slightly different: now the domain is  $0.53 \times 0.27 \text{ mm}^2$ , and the major and minor radii of the ellipse measure respectively  $53 \text{ }\mu\text{m}$  and  $21 \text{ }\mu\text{m}$ .

Fig. 6 shows the phase field evolution in the system as obtained with the two methods compared. The contours of the dendritic structures computed with both methods are similar. However, the ones obtained with the consistent method are more complex. This is probably due to the excessive dissipation of the midpoint rule, directly derived from its lack of energy conservation. Fig. 7 shows the temperature plots obtained with the two methods at several instants of the simulation. The differences between both solutions are difficult to appreciate, but the one obtained with the midpoint rule seems to have smeared some of the details available in the consistent solution.

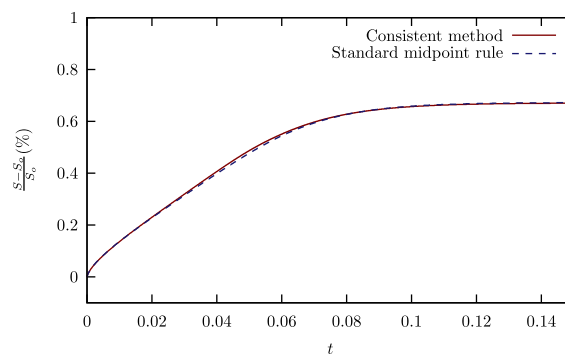


Fig. 9. Relative entropy evolution in Example 5.2.

The curves in Figs. 8 and 9 show the correct (physical) evolution in the solution obtained by the proposed method. On the other hand, the same figures show that the method based on the midpoint rule, although showing a remarkably non-negative entropy production, produces a non-physical energy loss. This additional energy dissipation, although apparently small, results in a clear different dendritic pattern, as illustrated in the phase field plot of the simulation at time  $t = 0.2$  s. From this figure it is apparent that the additional (non-physical) dissipation destroys part of the rich dendritic structures predicted by the consistent method.

In a final note, we observe that conserving schemes have been shown to be more robust than the midpoint rule, when applied to problems in solid and structural mechanics (see, e.g. [19–22]). In such problems, conserving schemes allowed, in general, for much larger time step sizes than the midpoint or the trapezoidal rule. We did not find, however, such a stability improvement in the problems simulated in the current work. A possible reason for it is that in solid mechanics discrete models are typically stiff, and conserving methods provide algorithmic control over the growth of unresolved high frequency modes. Wang's model of solidification is intrinsically dissipative, and oscillations seem to be well taken care of by the model itself, without need for additional control by the numerical method. In any case, even though the conservation/dissipation properties of the new method are strictly verified for every converged time step, it has time step size limitations like any other implicit time stepping algorithm.

## 6. Summary

In this work we have presented the formulation and analysis of a numerical method for the approximation of the solidification model of Penrose and Fife [1] and Wang et al. [2]. The method uses finite elements to discretize the equations in space and a midpoint-type integration in time. The result is a second-order accurate method in time which, most notably, strictly preserves the two laws of thermodynamics.

The merits of the proposed method are threefold. First, the method delivers second order (in time) approximate solutions to solidification problems at a computational cost which is comparable to that of the standard midpoint rule, but with enhanced qualitative properties, namely, the preservation of the two laws of thermodynamics. Second, we have proved analytically that the new method inherits the Lyapunov stability of the continuum problem, in contrast with the midpoint rule. Third, the numerical examples presented further seem to indicate that preserving the thermodynamic laws allows for a richer resolution of the dendritic structures that appear during solidification processes.

The formulation presented furnishes an example of a thermodynamically consistent method [8–10], the sole general purpose structure preserving discretization strategy known to the authors. In contrast with previous applications of such formulations, the proposed method lies outside the field of solid mechanics, where the ideas were initially presented.

## Acknowledgements

B. Gonzalez-Ferreiro and I. Romero acknowledge the financial support from the Spanish Ministry of Science and Innovation under Grants DPI2009-14305-C02-02 and DPI2012-36429.

H. Gomez gratefully acknowledges the funding provided by Xunta de Galicia (Grants #09REM005118PR and #09MDS00718PR), Ministerio de Ciencia e Innovación (Grants #DPI2009-14546-C02-01 and #DPI2010-16496) cofinanced with FEDER funds, and Universidad de A Coruña.

## References

- [1] Penrose O, Fife PC. Thermodynamically consistent models of phase-field type for the kinetic of phase transitions. *Physica D* 1990;43(1):44–62.
- [2] Wang S-L, Sekerka RF, Wheeler AA, Murray BT, Coriell SR, Braun RJ, et al. Thermodynamically-consistent phase-field models for solidification. *Physica D* 1993;69(1–2):189–200.

- [3] Stefan J. Über einige probleme der theorie der wärmeleitung. Sitzungsber Wiener Akad Math Naturwiss Abt 1889;98:173–484.
- [4] Gibbs JW. Collected works. Yale University Press; 1948.
- [5] Kobayashi R. Modeling and numerical simulations of dendritic crystal growth. *Physica D* 1993;63:410–23.
- [6] Caginalp G, Eck C. Rapidly converging phase field models via second order asymptotics. *Discrete Contin Dyn – B* 2005;142–52.
- [7] Chen X, Caginalp G, Eck C. A rapidly converging phase field model. *Discrete Contin Dyn – A* 2006;15(4):1017–34.
- [8] Romero I. Thermodynamically consistent time stepping algorithms for nonlinear thermomechanical systems. *Int J Numer Methods Eng* 2009;79(6):706–32.
- [9] Romero I. Algorithms for coupled problems that preserve symmetries and the laws of thermodynamics. Part I: monolithic integrators and their application to finite strain thermoelasticity. *Comput Methods Appl Mech Eng* 2010;199:1841–58.
- [10] Romero I. Algorithms for coupled problems that preserve symmetries and the laws of thermodynamics. Part II: fractional step methods. *Comput Methods Appl Mech Eng* 2010;199:2235–48.
- [11] García Orden JC, Romero I. Energy-Entropy-Momentum integration of discrete thermo-visco-elastic dynamics. *Eur J Mech A – Solid* 2012;32:76–87.
- [12] Labudde RA, Greenspan D. Energy and momentum conserving methods of arbitrary order for the numerical integration of equations of motion – I. Motion of a single particle. *Numer Math* 1976;25:323–46.
- [13] Labudde RA, Greenspan D. Energy and momentum conserving methods of arbitrary order for the numerical integration of equations of motion – II. Motion of a system of particles. *Numer Math* 1976;26:1–16.
- [14] Gotusso L. On the energy theorem for the Lagrange equations in the discrete case. *Appl Math Comput* 1985;17(2):129–36.
- [15] Itoh T, Abe K. Hamiltonian-conserving discrete canonical equations based on variational difference quotients. *J Comput Phys* 1988;76:85–102.
- [16] Gonzalez O. Time integration and discrete Hamiltonian systems. *J Nonlinear Sci* 1996;6:449–67.
- [17] Gonzalez O. Design and analysis of conserving integrators for nonlinear Hamiltonian systems with symmetry [Ph.D. thesis]. Stanford University, 1996.
- [18] Simo JC, Wong K. Unconditionally stable algorithms for rigid body dynamics that exactly preserve energy and momentum. *Int J Numer Methods Eng* 1991;31:19–52.
- [19] Simo JC, Tarnow N. The discrete energy-momentum method. Conserving algorithms for nonlinear elastodynamics. *Z Angew Math Phys* 1992;43(5):757–92.
- [20] Simo JC, Tarnow N, Wong KK. Exact energy-momentum conserving algorithms and symplectic schemes for nonlinear dynamics. *Comput Methods Appl Mech Eng* 1992;100(1):63–116.
- [21] Betsch P, Steinmann P. Conservation properties of a time FE method. Part I: time-stepping schemes for N-body problems. *Int J Numer Methods Eng* 2000;49:599–638.
- [22] Romero I, Armero F. An objective finite element approximation of the kinematics of geometrically exact rods and its use in the formulation of an energy-momentum conserving scheme in dynamics. *Int J Numer Methods Eng* 2002;54(12):1683–716.
- [23] Betsch P, Uhlar S. Energy-momentum conserving integration of multibody dynamics. *Multibody Syst Dyn* 2007;17:243–9.
- [24] Furihata D. A stable and conservative finite difference scheme for the Cahn–Hilliard equation. *Numer Math* 2001;87(4):675–99. <http://dx.doi.org/10.1007/PL00005429>.
- [25] Hu Z, Wise SM, Wang C, Lowengrub JS. Stable and efficient finite-difference nonlinear-multigrid schemes for the phase field crystal equation. *J Comput Phys* 2009;228(15):5323–39.
- [26] Baskaran A, Hu Z, Lowengrub JS, Wang C, Wise SM, Zhou P. Energy stable and efficient finite-difference nonlinear multigrid schemes for the modified phase field crystal equation. *J Comput Phys* 2013;250:270–92.
- [27] Du Q, Nicolaides RA. Numerical analysis of a continuum model of phase transition. *SIAM J Numer Anal* 1991;28(5):1310–22.
- [28] Wu X, van Zwieten GJ, van der Zee KG. Stabilized second-order convex splitting schemes for Cahn–Hilliard models with application to diffuse-interface tumor-growth models. *Int J Numer Methods Biomed Eng*. <http://dx.doi.org/10.1002/cnm.2597>.
- [29] Gomez H, Hughes TJR. Provably unconditionally stable, second-order time-accurate, mixed variational methods for phase-field models. *J Comput Phys* 2011;230(13):5310–27.
- [30] Liu J, Gomez H, Evans JA, Hughes TJR, Landis CM. Functional entropy variables: a new methodology for deriving thermodynamically consistent algorithms for complex fluids, with particular reference to the isothermal Navier–Stokes–Korteweg equations. *J Comput Phys* 2013;248:47–86.
- [31] Guillén-González F, Tierra G. On linear schemes for a Cahn–Hilliard diffuse interface model. *J Comput Phys* 2013;234:140–71.
- [32] Galenko PK, Gomez H, Kropotin NV, Elder KR. Unconditionally stable method and numerical solution of the hyperbolic phase-field crystal equation. *Phys Rev E* 2013;88:013310.
- [33] McLachlan RI, Quispel GRW, Robidoux N. Geometric integration using discrete gradients. *Philos Trans R Soc London A* 1999;357:1021–45.
- [34] Sansour C, Wriggers P, Sansour J. On the design of energy-momentum integration schemes for arbitrary continuum formulations. Applications to classical and chaotic motion of shells. *Int J Numer Methods Eng* 2004;60:2419–40.
- [35] Bui QV. On the enforcing energy conservation of time finite elements for discrete elasto-dynamics problems. *Int J Numer Methods Eng* 2007;70(2):127–62.
- [36] Romero I. An analysis of the stress formula for energy-momentum methods in nonlinear elastodynamics. *Comput Mech* 2012;50:603–10.
- [37] Wheeler AA, Murray BT, Schaefer RJ. Computation of dendrites using a phase field model. *Physica D* 1993;66(1–2):243–62.